Critical exponents for branching annihilating random walks with an even number of offspring

Iwan Jensen*
Department of Mathematics, The University of Melbourne, Parkville, Victoria 3052, Australia
(Received 9 May 1994)

Recently, Takayasu and Tretyakov [Phys. Rev. Lett. **68**, 3060 (1992)] studied branching annihilating random walks (BAW's) with $n = 1$–5 offspring. These models exhibit a continuous phase transition to an absorbing state. For odd n the models belong to the universality class of directed percolation. For even n the particle number is conserved modulo 2 and the critical behavior is not compatible with directed percolation. In this article I study the BAW with $n = 4$ using time-dependent simulations and finite-size scaling, obtaining precise estimates for various critical exponents. The results are consistent with the conjecture: $\beta/\nu_\perp = \frac{1}{2}$, $\nu_\parallel/\nu_\perp = \frac{7}{4}$, $\gamma = 0$, $\delta = \frac{2}{7}$, $\eta = 0$, and $\delta_h = \frac{9}{2}$. These critical exponents characterize, respectively, the dependence of the order parameter $(\beta/\nu_\perp)$ and relaxation time $(\nu_\parallel/\nu_\perp)$ on system size, the growth of fluctuations (γ) close to the critical point, the long-time behavior of the probability of survival (δ) and average number of particles (η) when starting at time zero with just two particles, and finally the decay of the order parameter (δ_h) at the critical point in the presence of an external source.

PACS number(s): 05.70.Ln, 05.50.+q, 64.90.+b

I. INTRODUCTION

Extensive studies of various nonequilibrium models exhibiting a second-order phase transition to a *unique* absorbing state have revealed that directed percolation (DP) [1–4] is the generic critical behavior of such models. Other well-known models belonging to the DP universality class are the contact process [5–7], Schlögl's first and second models [8–11], and Reggeon field theory [9,12]. Numerous models studied in recent years demonstrate the robustness of this universality class against a wide range of changes in the local kinetic rules such as multiparticle processes [13–16], diffusion [17], and changes in the number of components [18]. Very recently it was shown that even models with infinitely many absorbing states may exhibit DP critical behavior [19].

Recently, Takayasu and Tretyakov [20] studied the branching annihilating random walk (BAW) with $n = 1$–5 offspring. The BAW is a lattice model in which each site is either empty or occupied by a single particle. The evolution rules are quite simple and each "elementary" step starts by chosing a particle at random. With probability p the particle jumps to a randomly chosen nearest neighbor. If this site is already occupied the particles annihilate mutually. With probability $1 - p$ the particle produces n offspring, which are placed on the closest neighboring sites. When an offspring is created on a site already occupied, both particles annihilate leaving behind an empty site. In one dimension (1D) for $n = 1$ it has been shown [21] that the BAW has an active steady-state for sufficiently small p. Computer simulations revealed that the phase transition from the active state to the absorbing state is continuous [20]. BAW's with an odd number of offspring include a combination of diffusion and various multiparticle processes. One would expect, therefore, bearing in mind the robustness of DP critical behavior, that the transition should belong to the universality class of directed percolation. The steady-state concentration of particles $\bar{\rho}$ (which is the appropriate order parameter) decays as

$$\bar{\rho} \propto |p_c - p|^\beta, \tag{1}$$

in the supercritical regime $(p < p_c)$, where β is the order parameter critical exponent. Estimates for β, obtained from computer simulations, were however only marginally consistent with directed percolation. Takayasu and Tretyakov [20] found $p_c = 0.108 \pm 0.001$ and $\beta = 0.32 \pm 0.01$ which should be compared to the value $\beta = 0.2769 \pm 0.0002$ [22] for the one-dimensional contact process. For $n = 3$ and $n = 5$ they found that $p_c = 0.461 \pm 0.002$ and 0.718 ± 0.001, respectively, with $\beta = 0.33 \pm 0.01$ in both cases. Time-dependent computer simulations [23] for $n = 1$ and 3 yielded estimates for three critical exponents in good agreement with directed percolation, thus supporting the notion that BAW's with an odd number of offspring belong to the DP universality class. This conclusion has been confirmed recently by a study [24] of the BAW with $n = 1$ yielding a value of β consistent with DP, using mean field cluster expansions and the coherent anomaly method [25].

When n is *even* the number of particles is conserved modulo 2 and the absorbing state can only be reached if one initially has an even number of particles. For $n = 2$ the model does not have an active steady state [26,27] whereas for $n = 4$ it was found [20] that $p_c = 0.72 \pm 0.01$ and $\beta = 0.7 \pm 0.1$, which clearly places the model outside the DP universality class. Grassberger *et al.* [28] studied a model, involving the processes $X \to 3X$ and $2X \to 0$, from which it is obvious that once again the number of particles is conserved modulo 2. Steady-state and time-dependent computer simulations yielded non-DP values for various critical exponents (this model and the results will be described in more detail in Sec. VI). The conservation of particle number modulo 2 is probably responsible

*Electronic address: iwan@maths.mu.oz.au

for the non-DP behavior. Support for this idea was provided by a recent study [29] of a modified version of the BAW with $n = 4$. In this study, spontaneous annihilation of particles was included, thus destroying the conservation of particles modulo 2. Results from computer simulations clearly showed that adding spontaneous annihilation changes the critical behavior from non-DP to DP, even for very low rates of spontaneous annihilation [29].

As non-DP behavior is so rare it is clearly of great interest to study BAW's with an even number of offspring in greater detail. In this paper, I present results from extensive computer simulations of the one-dimensional BAW with $n = 4$ using time-dependent simulations and finite-size scaling analysis of steady-state simulations.

II. TIME-DEPENDENT SIMULATIONS

Earlier studies [4,9,15,16,30] have revealed that time-dependent simulation is a very efficient method for determining critical points and exponents for models with a continuous transition to an absorbing state. The general idea of time-dependent simulations is to start from a configuration that is very close to the absorbing state, and then follow the "average" time evolution of this configuration by simulating a large ensemble of independent realizations. In the simulations presented here, I always started, at $t = 0$, with two occupied nearest neighbor sites placed at the origin. I then made a number N_S of independent runs, typically 5×10^5, for different values of p in the vicinity of p_c. As the number of particles is very small an efficient algorithm may be devised by keeping a list of occupied sites. In each elementary step a particle is draw at random from this list and the processes are performed according to the rules given earlier. Before each elementary change, the time variable is incremented by $1/n(t)$, where $n(t)$ is the number of particles on the lattices prior to the change. This makes one time step equal to (on the average) one attempted update per lattice site. Each run had a maximal duration t_M of 5000 time steps. I measured the survival probability $P(t)$ (the probability that the system had not entered the absorbing state at time t), the average number of occupied sites $\bar{n}(t)$, and the average mean square distance of spreading $\bar{R}^2(t)$ from the center of the lattice. Notice that $\bar{n}(t)$ is averaged over all runs whereas $\bar{R}^2(t)$ is averaged only over the surviving runs. From the scaling ansatz for the contact process and similar models [4,9,30] it follows that the quantities defined above are governed by power laws at p_c as $t \to \infty$

$$P(t) \propto t^{-\delta}\Phi(\Delta t^{1/\nu_\parallel}), \tag{2}$$

$$\bar{n}(t) \propto t^{\eta}\Psi(\Delta t^{1/\nu_\parallel}), \tag{3}$$

$$\bar{R}^2(t) \propto t^{z}\Theta(\Delta t^{1/\nu_\parallel}), \tag{4}$$

where $\Delta = |p_c - p|$ is the distance from the critical point and $\nu_\parallel$ is the correlation length exponent in the time direction.

If the scaling functions Φ, Ψ, and Θ are nonsingular at the origin it follows that $P(t)$, $\bar{n}(t)$, and $\bar{R}^2(t)$ behave as pure power laws at p_c for $t \to \infty$. In log-log plots of $P(t)$, $\bar{n}(t)$, and $\bar{R}^2(t)$ as a function of t one should see (asymptotically) a straight line at $p = p_c$. The curves will show positive (negative) curvature when $p < p_c$ ($p > p_c$). This enables one to obtain accurate estimates for p_c. The asymptotic slope of the (critical) curves define the dynamic critical exponents δ, η, and z. Generally one has to expect corrections to the pure power-law behavior so that $P(t)$ is more accurately given as [4]

$$P(t) \propto t^{-\delta}(1 + at^{-1} + bt^{-\delta'} + \cdots) \tag{5}$$

and similarly for $\bar{n}(t)$ and $\bar{R}^2(t)$. More precise estimates for the critical exponents can be obtained by looking at local slopes

$$-\delta(t) = \frac{\ln[P(t)/P(t/m)]}{\ln(m)}, \tag{6}$$

and similarly for $\eta(t)$ and $z(t)$; in this work I used $m = 5$. The local slope $\delta(t)$ behaves as [4]

$$\delta(t) = \delta + at^{-1} + b\delta' t^{-\delta'} + \cdots \tag{7}$$

and similar expressions for $\eta(t)$ and $z(t)$. Thus in a plot of the local slopes vs $1/t$ the critical exponents are given by the intercept of the curves for p_c with the y axis. The off-critical curves often have a very notable curvature, i.e., one will see the curves for $p > p_c$ veering downward while the curves for $p < p_c$ veer upward.

The local slopes thus provide us with a very efficient means for estimating both the location of the critical point and the values of various critical exponents. In Fig. 1, I have plotted the local slopes for various values of p. The maximal number of time steps $t_M = 5000$ and the number of samples $N_S = 5 \times 10^5$ except for $p = 0.721$ where $N_S = 2 \times 10^6$. One clearly sees that the curves for $p = 0.715$ veer upwards and the curves for $p = 0.727$ veer downward and these values of p are thus off critical. For $p = 0.724$ the curve for $-\delta(t)$ veers downward at the end as $1/t \to 0$. I, therefore, conclude that $p_c < 0.724$. The curve for $p = 0.718$ does not exhibit pronounced curvature and is thus close to p_c, however $\eta(t)$ does seem to veer upwards so p_c is probably larger than 0.718. All in all it seems that $p = 0.721$ is the value closest to p_c leading to the estimate $p_c = 0.721 \pm 0.003$, which is in excellent agreement with the estimate $p_c = 0.72 \pm 0.01$ obtained by Takayasu and Tretyakov [20]. In order to obtain a better estimate for p_c and the critical exponents I performed extensive simulations for $p = 0.7210$, 0.7215, and 0.7220, with $t_M = 5000$ and $N_S = 2 \times 10^6$. The resulting local slopes are shown in Fig. 2. None of the curves exhibit pronounced curvature, however, the estimate $\eta = 0$ obtained for $p = 0.7215$ is to be preferred (if only for aesthetical reasons) over an estimate that is very close to zero. All in all, I conclude that $p_c = 0.7215 \pm 0.0005$. From the intercept of the critical curves with the y axis I obtain the estimates $\delta = 0.286 \pm 0.001$, $\eta = 0 \pm 0.001$, and $z = 1.143 \pm 0.003$. These results certainly suggest that $\eta = 0$ is an *exact* result. One might thus hope that the other exponents are given by simple fractions, and indeed

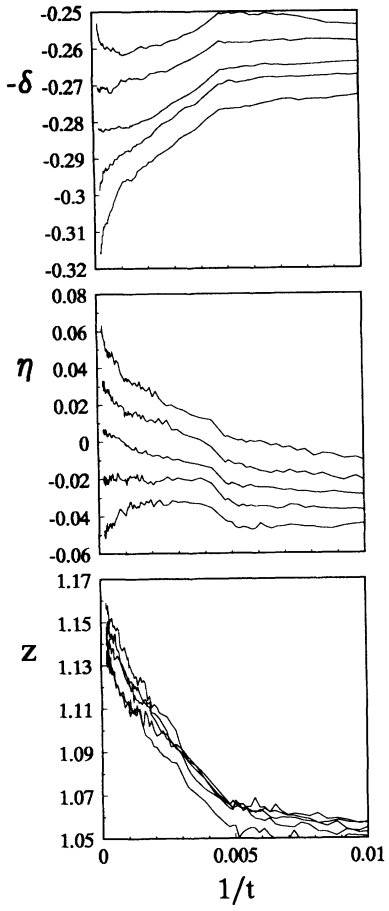

FIG. 1. Local slopes $-\delta(t)$ (upper panel), $\eta(t)$ (middle panel), and $z(t)$ (lower panel), as defined in Eq. 6 with $m = 5$. Each panel contains five curves with, from top to bottom, $p = 0.715$, 0.718, 0.721, 0.724, and 0.727.

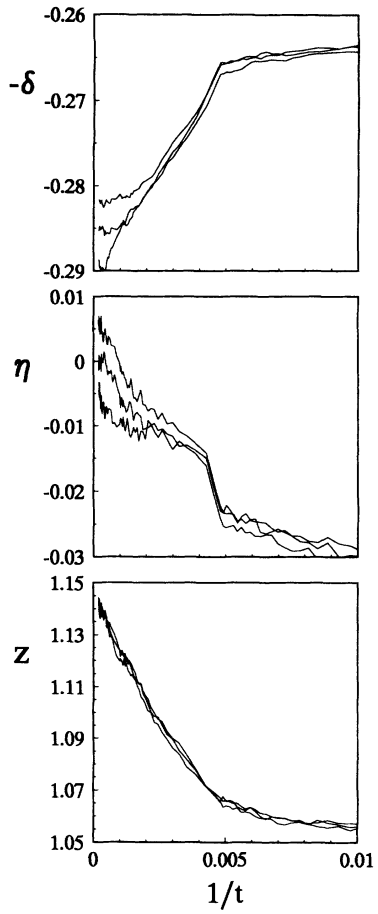

FIG. 2. Same as in Fig. 1 but for $p = 0.7210$, 0.7215, and 0.7220.

I find that $\delta = \frac{2}{7} = 0.28571\ldots$ and $z = \frac{8}{7} = 1.142\,85\ldots$ are consistent with the simulation results. Note that both the conjectured exact values and the estimates obey the hyperscaling relation [4,9,30]

$$4\delta + 2\eta = dz, \tag{8}$$

which lends further support to the validity of the asumptions made above.

III. FINITE-SIZE SCALING ANALYSIS

The concepts of finite-size scaling [31], though originally developed for equilibrium systems, are also applicable to nonequilibrium second-order phase transitions. Aukrust *et al.* [14] showed how finite-size scaling can be used very successfully to study the critical behavior of nonequilibrium systems exhibiting a continuous phase transition to an absorbing state. As in equilibrium second-order phase transitions one assumes that the (infinite-size) nonequilibrium system features length and time scales that diverge at criticality as

$$\xi(p) \propto |p_c - p|^{-\nu_\perp}, \tag{9}$$

and

$$\tau(p) \propto |p_c - p|^{-\nu_\parallel}, \tag{10}$$

where $\nu_\perp$ ($\nu_\parallel$) is the correlation length exponent in the space (time) direction.

A. Static behavior

One expects finite-size effects to become important when the correlation length $\xi(p) \sim L$. The basic finite-size scaling ansatz is that various physical quantities depend on system size only through the scaled length $L/\xi(p)$, or equivalently through the variable $(p_c - p)L^{1/\nu_\perp}$. Thus we assume that the order parameter depends on system size and distance from the critical point as

$$\rho_s(p, L) \propto L^{-\beta/\nu_\perp} f((p_c - p)L^{1/\nu_\perp}), \tag{11}$$

such that at p_c

$$\rho_s(p_c, L) \propto L^{-\beta/\nu_\perp}, \tag{12}$$

and $f(x) \propto x^{\beta}$ for $x \to \infty$, so that Eq. (1) is recovered when $L \to \infty$ in the critical region. In ρ_s, and other quantities, the subscript s indicates an average taken over the *surviving* samples, i.e., the average includes only those samples that have not yet entered the absorbing state. The restriction to surviving samples ensures that the system enters a "quasisteady state" in which a quantity such as ρ_s becomes constant after a relative short transient time [14,19]. In the supercritical regime ρ_s should approach a nonzero asymptote for $L \gg \xi(p)$, while in the subcritical regime one expects ρ_s to decay faster than a power law. Thus p_c may be determined as the value yielding a straight line in a log-log plot of ρ_s versus L. However, since the time-dependent simulations already yielded an accurate estimate of p_c, I have only performed the steady-state simulations for $p = p_c = 0.7215$ with various values of the system size L. Figure 3 shows a log-log plot of the average concentration of particles $\rho_s(p_c, L)$ in the quasisteady state as a function of L. The number of time steps t_M and independent samples N_S varied from $t_M = 200$, $N_S = 200\,000$ for $L = 16$ to $t_M = 5000\,000$, $N_S = 100$ for $L = 16384$. As can be seen the data falls very nicely on a straight line, from the slope of this line I obtain the estimate $\beta/\nu_\perp = 0.50 \pm 0.01$. This result clearly suggests that $\beta/\nu_\perp = \frac{1}{2}$.

Another exponent estimate can be obtained from the fluctuations,

$$\bar{\chi} = L^d(\langle \rho^2 \rangle - \langle \rho \rangle^2) \propto |p_c - p|^{-\gamma}, \tag{13}$$

where L is the linear extension of the system. Equation (13) thus leads to the following finite-size scaling ansatz:

$$\chi_s(p, L) \propto L^{\gamma/\nu_\perp} g((p_c - p)L^{1/\nu_\perp}), \tag{14}$$

and

$$\chi_s(p_c, L) \propto L^{\gamma/\nu_\perp}. \tag{15}$$

When plotting the data for χ on a log-log scale the curve had no pronounced slope showing that $\gamma \simeq 0$ suggesting that the fluctuations grow only logarithmically with system size. Figure 4 shows a log-lin plot of the susceptibility $\chi_s(p_c, L)$ as a function of L. The data falls more or less on a straight line (with large error bars for large L values) showing that γ indeed is zero. Note that this result through the scaling relation [14,19]

$$\gamma = d\nu_\perp - 2\beta, \tag{16}$$

leads to the *exact* result $\beta/\nu_\perp = \frac{1}{2}$ in full agreement with the simulation results for ρ_s.

B. Dynamical behavior

Additional exponents may be obtained from the dynamical behavior of the system. In this study, I define a characteristic time, $\tau(p, L)$, as the time it takes for one half the sample to enter the absorbing state. From Eq. (10) we obtain the following finite-size scaling form:

$$\tau(p, L) \propto L^y h((p_c - p)L^{1/\nu_\perp}), \tag{17}$$

where $y = \nu_\parallel/\nu_\perp$. At p_c we thus have

$$\tau(p_c, L) \propto L^y. \tag{18}$$

In Fig. 5, I have plotted, on a log-log scale, $\tau_s(p_c, L)$ as a function of L. Again we see a nice straight line this time with slope $\nu_\parallel/\nu_\perp = 1.75 \pm 0.01$, which leads to the conjecture $\nu_\parallel/\nu_\perp = \frac{7}{4}$. This value agrees with the scaling relation [4],

$$z = 2\nu_\perp/\nu_\parallel. \tag{19}$$

One may also study the dynamical behavior by looking at the time dependence of $\rho_s(p_c, L, t)$. For $t \gg 1$ and $L \gg 1$ one can assume a scaling form

$$\rho_s(p_c, L, t) \propto L^{-\beta/\nu_\perp} f(t/L^y). \tag{20}$$

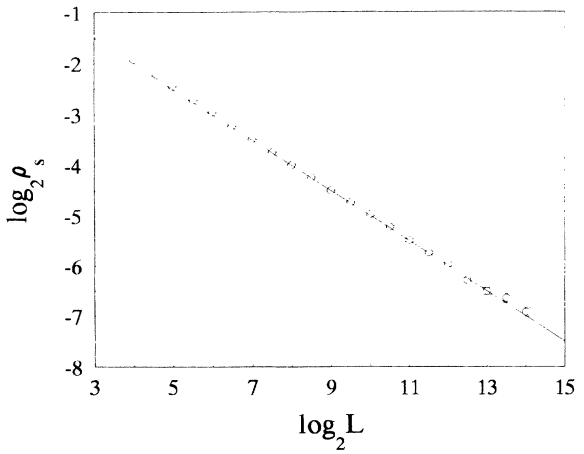

FIG. 3. $\rho_s(p_c, L)$ vs L at $p_c = 0.7215$. The slope of the line is $\beta/\nu_\perp = \frac{1}{2}$.

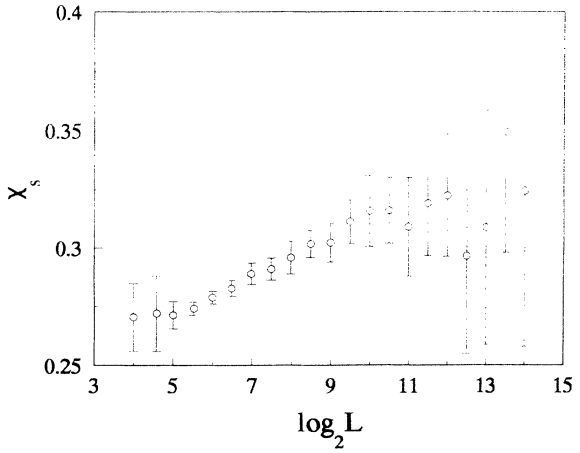

FIG. 4. Log-lin plot of the susceptibility $\chi_s(p_c, L)$ vs L at the critical point $p_c = 0.7215$.

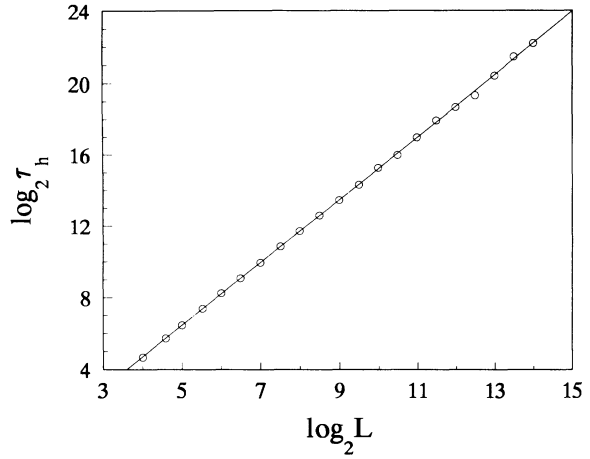

FIG. 5. $\tau(p_c, L)$ vs L with $p_c = 0.7215$. The slope of the line is $y = \nu_{\|}/\nu_{\perp} = \frac{7}{4}$.

At p_c the system shows power-law behavior for $t < L^y$ before finite-size effects become important. Thus for $L \gg 1$ and $t < L^y$, $\rho(p_c, L, t) \propto t^{-\theta}$. From Eq. (20) it then follows that

$$\theta = \beta/(\nu_{\perp} y) = \beta/\nu_{\|} = \delta. \tag{21}$$

Figure 6 shows the short-time evolution of the concentration of particles at p_c. The slope of the line drawn in the figure is $\theta = \frac{2}{7}$ and this value seems to be in excellent accord with the simulation data.

IV. DETERMINING β, $\nu_{\|}$, AND $\nu_{\perp}$

The numerical values of $\nu_{\|}$ and $\nu_{\perp}$ turns out to be quite large. It is, therefore, difficult to obtain accurate estimates for these exponents and β since the correlation time and length grow rapidly as one approaches the critical point. The exponent estimates presented in this section are thus marked by far greater uncertainties than those of the preceding sections.

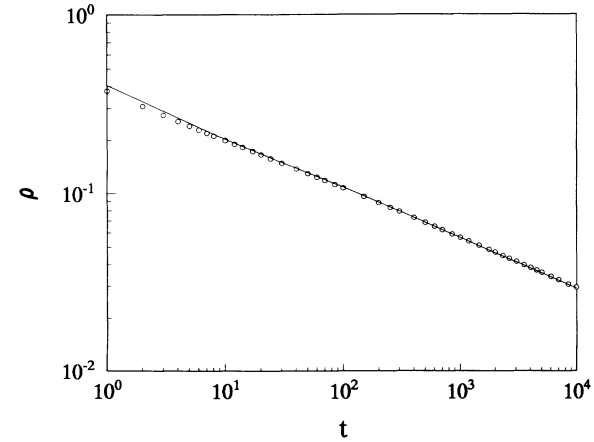

FIG. 6. The short-time decay of the density of particles $\rho(p_c, L, t)$ as a function of t at the critical point with $L = 2^{15}$. The slope of the line is $\theta = \beta/\nu_{\|} = \frac{2}{7}$.

A. Time-dependent simulations

Estimates for β and $\nu_{\|}$ can be obtained from time-dependent simulations in the supercritical and subcritical regions [30]. In the *supercritical* region the number of indepent runs N_S and the maximal duration t_M of each run varied from $N_S = 15000$, $t_M = 1000\,000$ closest to p_c, to $N_S = 100000$, $t_M = 100$ furthest away from p_c. One may analyze the data by utilizing the scaling behavior expressed in Eqs. (2)–(4). First we rewrite the equations by changing the variable to $x = \Delta t^{1/\nu_{\|}}$. The expression for the survival probability then becomes (after noting that $t^{-\delta} = \Delta^{\nu_{\|}\delta} x^{-\nu_{\|}\delta}$)

$$P(x) \propto \Delta^{\nu_{\|}\delta} x^{-\nu_{\|}\delta} \Phi(x). \tag{22}$$

The expressions for $\bar{n}(t)$ and $\bar{R}^2(t)$ can be rewritten in a similar manner. In plots of $\Delta^{-\nu_{\|}\delta} P(t)$, $\Delta^{\nu_{\|}\eta} \bar{n}(t)$, or $\Delta^{\nu_{\|} z} \bar{R}^2(t)$ vs x we should see the data collapse onto single curves. Since I am fairly certain that the estimates for p_c, δ, η, and z are very accurate there is really only one free variable $\nu_{\|}$ to be determined in the scaling analysis. Figure 7 shows the results with $p_c = 0.7215$, $\delta = \frac{2}{7}$, $\eta = 0$, and $z = \frac{8}{7}$, while the "free" variable $\nu_{\|} = 3.25$, which leads to a decent data collapse. The curves that do not collapse onto the common curve are those furthest away from p_c and thus those for which corrections to scaling are expected to be the strongest. The value $\nu_{\perp} = 3$ also leads to a decent collapse, but now the deviating curves are those closest to p_c which should rule out this value. $\nu_{\|} = 3.5$ is also a possibility, but the scaling collapse is less impressive in this case. Due to the fact that the simulations could not be extended closer to p_c (the demands in CPU time simply become too great) it is not possible to rule this value out entirely. I thus conclude that $\nu_{\|} = 3.25 \pm 0.25$ though the lower end of this range is highly unlikely. Using the finite-size results $\nu_{\|}/\nu_{\perp} = \frac{7}{4}$ and $\beta/\nu_{\perp} = \frac{1}{2}$, we see that $\nu_{\|} = \frac{13}{4}$ gives the estimates $\nu_{\perp} = \frac{13}{7}$ and $\beta = \frac{13}{14}$, whereas $\nu_{\|} = \frac{7}{2}$ yields $\nu_{\perp} = 2$ and $\beta = 1$. The latter set of values is certainly aesthetically more appealing, but as I will argue below the simulations do seem to favor the former values.

β and $\nu_{\|}$ can also be estimated directly from the asymptotic behavior of $P(t)$ and $\bar{n}(t)$. We see that by setting $\phi(y) = y^{-\delta\nu_{\|}} \Phi(y)$ we may rewrite Eq. (2) as

$$P(t) \propto \Delta^{\nu\delta} \phi(\Delta t^{1/\nu_{\|}}). \tag{23}$$

Since the system is in the supercritical region there must be a finite chance of survival; were this not the case any configuration would eventually die out, contrary to our knowledge that the system has an active steady state in this regime. Thus since $P_\infty \equiv \lim_{t\to\infty} P(t)$ is finite, $\lim_{y\to\infty} \psi(y)$ is finite too, and we get

$$P_\infty \propto \Delta^{\nu_{\|}\delta}. \tag{24}$$

For the contact process it has been shown [9] that P_∞ and the average steady-state concentration of particles $\bar{\rho}$ are governed by the same critical exponent. Numerical studies have shown that this also holds for a wide variety of other models. Assuming that this also is the case for the BAW, the following scaling relation should hold:

$$\beta = \nu_{||}\delta. \tag{25}$$

Figure 8 shows a log-log plot of the ultimate survival probability P_∞ as a function of the distance from the critical point. The slope of the curve yields the estimate $\beta = 0.93 \pm 0.05$.

Assuming that the density of the surviving events is constant inside a d-dimensional sphere expanding with constant velocity v, we find that

$$\langle \bar{R}^2(t)^{1/2} \rangle \approx \text{const} v \times t \tag{26}$$

for fixed $\Delta > 0$ and for $t \to \infty$. From Eq. (4) we see that $\langle \bar{R}^2(t) \rangle^{1/2} \propto t$ only if $g(y) \sim y^{(1-z/2)\nu_{||}}$ for $y \to \infty$, showing that

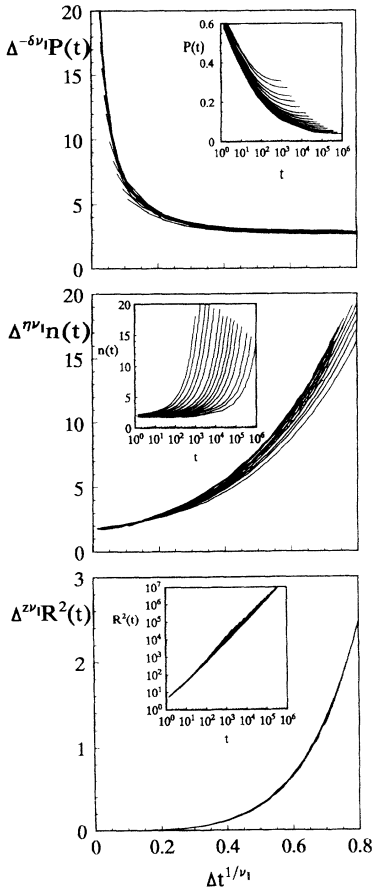

FIG. 7. Plots of $\Delta^{-\delta\nu_{||}}P(t)$ (upper panel), $\Delta^{\eta\nu_{||}}\bar{n}(t)$ (middle panel), and $\Delta^{z\nu_{||}}\bar{R}^2(t)$ (lower panel) vs $\Delta t^{1/\nu_{||}}$ for various values of p in the supercritical region. The critical parameters are $p_c = 0.7215$, $\nu_{||} = \frac{13}{4}$, $\delta = \frac{2}{7}$, $\eta = 0$, and $z = \frac{8}{7}$. In each panel is an inset showing the unscaled data, i.e., $P(t)$, $\bar{n}(t)$, and $\bar{R}^2(t)$ vs $1/t$.

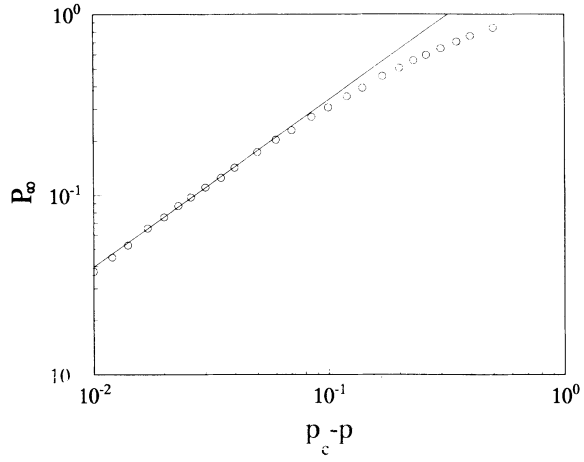

FIG. 8. The ultimate survival probability P_∞ vs $p_c - p$. The slope of the line is $\beta = \frac{13}{14}$.

$$v \propto \Delta^{(1-z/2)\nu_{||}}. \tag{27}$$

Thus, $R_\infty = \lim_{t\to\infty}\langle \bar{R}^2(t) \rangle^{1/2}/t \propto \Delta^{(1-z/2)\nu_{||}}$, so that we may obtain an estimate for the exponent $(1 - z/2)\nu_{||} = \nu_{||} - \nu_\perp$ from the asymptotic behavior of $\bar{R}^2(t)$. In Fig. 9, I have plotted R_∞ as a function of the distance from the critical point. The slope of the line yields $\nu_{||} - \nu_\perp = 1.35 \pm 0.10$.

Finally, we may find the asymptotic behavior of the average number of particles in the supercritical regime, as it is simply proportional to the product of the concentration of particles, the ultimate survival probability, and the volume of the sphere inside which the surviving events exist. Equations (26), (27), and (25) thus gives

$$\begin{aligned} \bar{n}(t) &\approx \text{const} \times \bar{\rho} P_\infty [\langle \bar{R}^2(t) \rangle^{1/2}]^d \\ &\sim \Delta^{2\beta+(1-z/2)\nu_{||}d}\, t^d. \end{aligned} \tag{28}$$

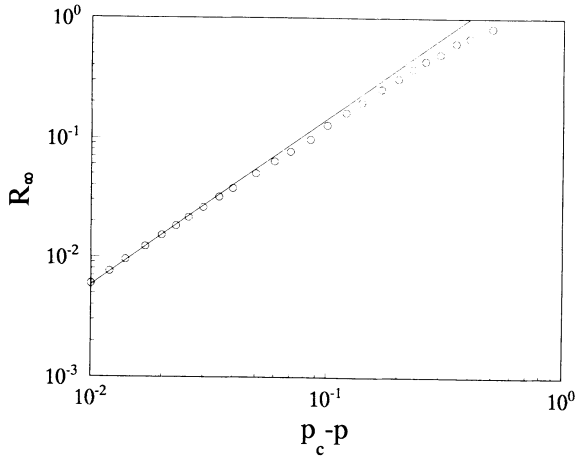

FIG. 9. $R_\infty = \lim_{t\to\infty}\langle \bar{R}^2(t) \rangle^{1/2}/t$ vs $p_c - p$. The slope of the line is $\nu_{||} - \nu_\perp = \frac{39}{28}$.

We thus see that $n_\infty = \lim_{t\to\infty} \bar{n}(t)/t^d \propto \Delta^{2\beta+(1-z/2)\nu_\parallel d}$. From the scaling relation Eq. (19) and the conjecture $\beta/\nu_\perp = \frac{1}{2}$ it follows that the critical exponent of n_∞ in 1D is $2\beta + (1 - z/2)\nu_\parallel = \nu_\parallel$. Figure 10 is a log-log plot of n_∞ vs $p_c - p$. From the asymptotic slope of the curve I estimate that $\nu_\parallel = 3.25 \pm 0.10$.

In the *subcritical* regime the process must eventually die, and since correlations are of finite range one expects $P(t)$ to decay *exponentially*. The associated scaling function must satisfy, $\Psi(y) \propto (-y)^{\delta\nu_\parallel} \exp[-b(-y)^{\nu_\parallel}]$for $y \to -\infty$, where b is a constant. When inserted in Eq. (2) this implies

$$P(t) \propto (-\Delta)^{\delta\nu_\parallel} \exp[-b(-\Delta)^{\nu_\parallel} t] \; . \tag{29}$$

Likewise, one expects that the average number of particles decays exponentially,

$$\bar{n}(t) \propto (-\Delta)^{-\eta\nu_\parallel} \exp[-c(-\Delta)^{\nu_\parallel} t]. \tag{30}$$

The decay constants in Eqs. (29) and (30) are just the inverse of the correlation time $\tau \propto \Delta^{-\nu_\parallel}$. We can thus find a corroborating estimate for $\nu_\parallel$ by studying the exponential decay of $P(t)$ and $\bar{n}(t)$ in the subcritical region. In Fig. 11, I have plotted the estimates for τ, obtained from the exponential decay of $\bar{n}(t)$, as a function of the distance from the critical point. The error-bars on these data points are so large that an improved estimate is out of the question. But clearly the value $\nu_\parallel = \frac{13}{4}$ is fully compatible with the data.

Since the population is not growing on average, we expect the surviving particles to spread through space via simple diffusion, which leads to $\Theta(y) \propto (-y)^{\nu_\parallel(1-z)}$ for $y \to -\infty$, which when inserted in Eq. (4) yields,

$$R^2_\infty = \lim_{t\to\infty} \bar{R}^2(t)/t \propto \Delta^{\nu_\parallel(1-z)}. \tag{31}$$

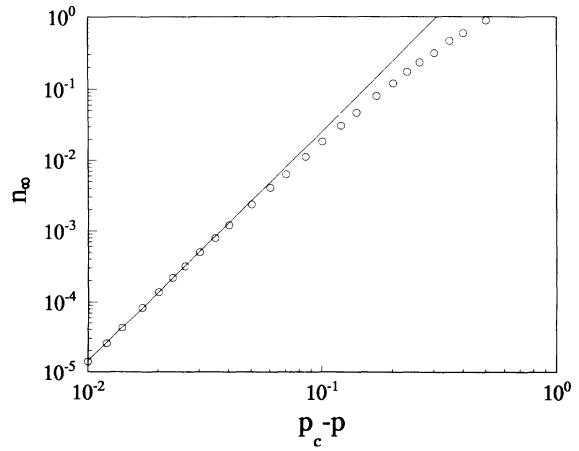

FIG. 10. The ultimate number of particles $n_\infty = \lim_{t\to\infty} \bar{n}(t)/t$ vs $p_c - p$. The slope of the line is $\nu_\parallel = \frac{13}{4}$.

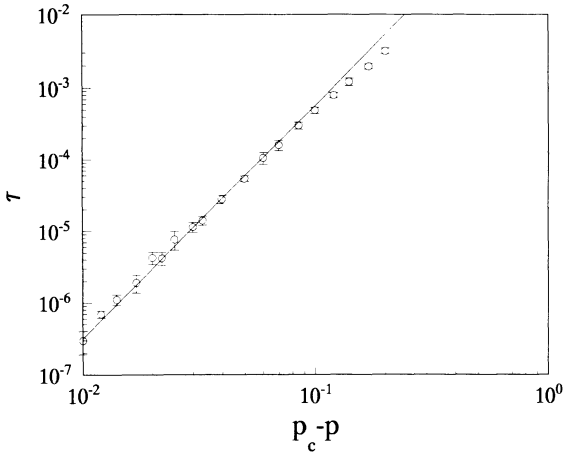

FIG. 11. The correlation time τ governing the decay of the number of particles vs $p - p_c$. The slope of the line is $\nu_\parallel = \frac{13}{4}$.

Figure 12 shows a log-log plot of R^2_∞ vs $p - p_c$. The slope of the line is $\nu_\parallel(1 - z) = \frac{13}{28}$, which agrees with the data, though again the spread of the data points is quite substantial.

B. Steady-state simulations

In Fig. 13, I have plotted $\bar{\rho}$ as a function of the distance from the critical point on a log-log scale, with $p_c = 0.7215$. The results were obtained by averaging over typically 100 independent samples. The number of time steps and system sizes varied from $t = 5000$, $L = 512$ far from p_c to $t = 500\,000$, $L = 8192$ closest to p_c. From the results I estimate that $\beta = 0.93 + (0.05)$ a value consistent with the conjecture $\beta = \frac{13}{14}$. Figure 14 shows a plot of $\bar{\chi}$ as a function of the distance from the critical point on a log-ln scale, with $p_c = 0.7215$. As can be seen the data clearly settles down to a constant close to the critical point thus confirming that $\gamma = 0$.

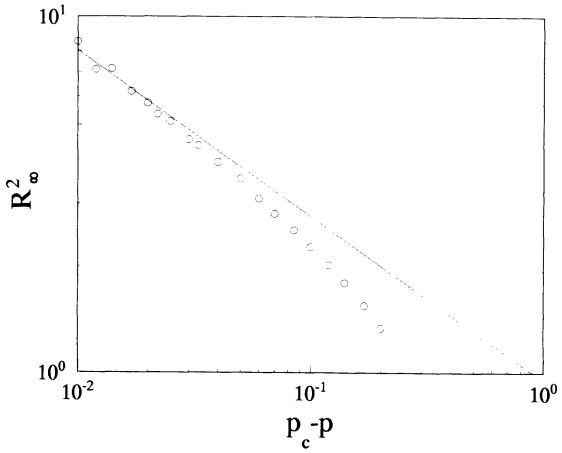

FIG. 12. Log-log plot of R^2_∞ vs $p - p_c$. The slope of the line is $\nu_\parallel(1 - z) = \frac{13}{28}$.

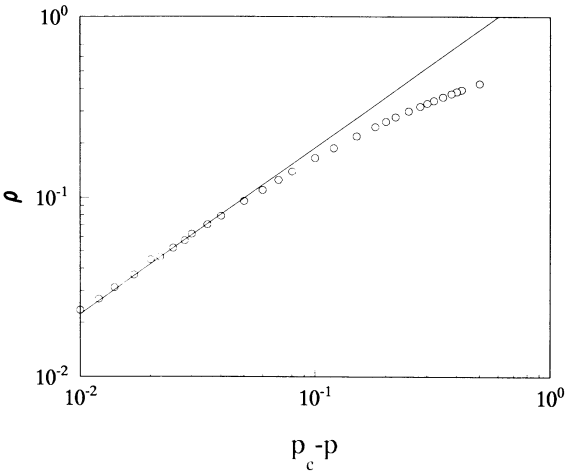

FIG. 13. The steady-state density of particles ρ vs $p_c - p$. The slope of the straight line is $\beta = \frac{13}{14}$.

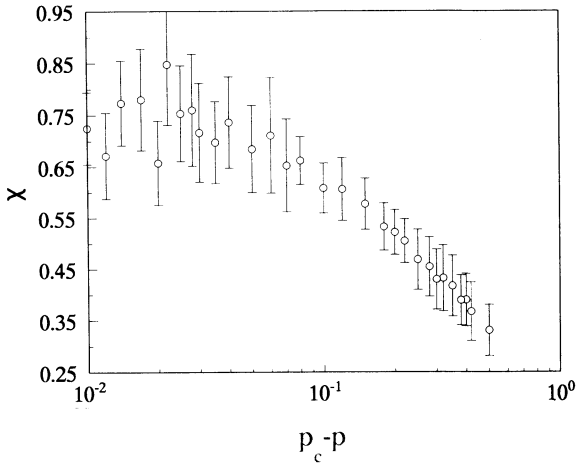

FIG. 14. The steady-state fluctuations in the number of particles χ vs the distance from the critical point.

V. FIELD EXPONENT

Finally, I examine the behavior in the presence of an external source h, which can be added simply by allowing pairs of nearest neighbor sites to become occupied *spontaneously* at rate h. Again, if a new particle is placed on an already occupied site the two particles annihilate mutually. This way of introducing the external source preserves the conservation of particles modulo 2. The diffusion and creation processes of the BAW now takes place at rates λ and unity, respectively, such that diffusion happens with probability $p = \lambda/(\lambda+h+1)$, creation with probabily $q = 1/(\lambda + h + 1)$, and spontaneous creation with probability $s = h/(\lambda + h + 1)$. The source removes the phase transition, just as an external magnetic field does in the Ising model. Since h is a second relevant parameter, one expects that at the critical point, $\lambda_c = p_c/(1-p_c) \simeq 2.5907$, the order parameter decreases as a power law when $h \to 0$

$$\bar{\rho} \propto h^{1/\delta_h}. \tag{32}$$

In Fig. 15, I have plotted the steady-state density of particles as a function of h at λ_c. The number of independent samples $N_S = 100$, the maximal number of time steps and system sizes varied from $t_M = 1000$, $L = 2048$ for large values of h to $t_M = 250\,000$, $L = 8192$ for small values of h. The data fit very nicely to a power law with exponent $1/\delta_h = 0.222 \pm 0.002$, which is consistent with the conjecture $\delta_h = \frac{9}{2}$.

VI. COMPARISON WITH OTHER STUDIES

Grassberger *et al.* [28] studied two one-dimensional cellular automata in which the number of kinks between ordered states is conserved modulo 2. Each site is in a state $S_i = 0, 1$ and the transition rules depend only on the site itself and its nearest neighbors. The model has the following evolution rules

$$\begin{array}{lccccccccccc} t: & 111 & 101 & 010 & 100 & 001 & \underbrace{\quad 011 \quad 110 \quad} & & 000 & & \\ t+1: & 0 & 0 & 1 & 1 & 1 & \begin{array}{l}0 \text{ with probability } p \\ 1 \text{ with probability } 1-p\end{array} & & 0 & & \text{model A} \end{array}$$

and

$$\begin{array}{lccccccccccc} t: & 111 & 101 & 010 & 100 & 001 & \underbrace{\quad 011 \quad 110 \quad} & & 000 & & \\ t+1: & 0 & 1 & 0 & 1 & 1 & \begin{array}{l}1 \text{ with probability } p \\ 0 \text{ with probability } 1-p\end{array} & & 0 & & \text{model B} \end{array}$$

When p is small the system orders itself spontaneously. In model A there are two symmetrical absorbing states consisting of alternating rows of 0 and 1. In model B the time-space pattern of the two absorbing states form a chessboard pattern [28]. When starting from a random initial configuration the system evolves to a state with small ordered domains separated by kinks. If p is small the density of kinks decreases to zero as the system evolves, but for $p > p_c$ a state with a nonzero density of kinks is reached. The evolution rules are such that the number of kinks is conserved modulo 2, this becomes much clearer by noting that the evolution rules for the kinks involve the two processes $X \to 3X$ and $2X \to 0$. Steady-state and time-dependent computer simulations

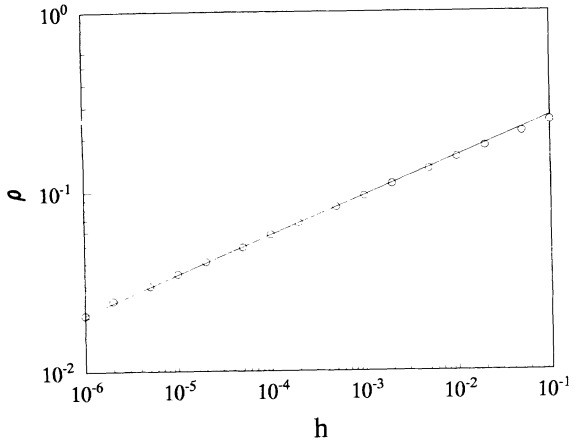

FIG. 15. The steady-state density of particles as a function of the external source h at the critical point $p_c = 0.7215$. The slope of the line is $1/\delta_h = \frac{2}{9}$.

yielded non-DP values for various critical exponents. In the time-dependent simulations of model B, Grassberger always started with a single kink so the absorbing state could never be reached and all trials survived indefinitely. The simulations yielded $p_c = 0.5403 \pm 0.0013$, $\eta = 0.272 \pm 0.012$, $z = 1.11 \pm 0.02$, $\nu_{\|} = 3.3 \pm 0.2$, and $\beta = 0.94 \pm 0.06$. Note that while η is very different from the results for the BAW, z is almost the same and both $\nu_{\|}$ and β are fully consistent with the estimates given above. This indicates that the two models belong to the same universality class, at least as far as the *static* critical behavior is concerned. The difference in the exponents obtained from time-dependent simulations are, however, simply due to the application of different initial configurations. By simulating the BAW with $n = 4$ starting with just one particle at the origin I obtained the estimates (see Fig. 16) $\eta = 0.282 \pm 0.005$ and $z = 1.140 \pm 0.005$, in excellent agreement with Grassberger's results. It is thus clear that the two models belong to the same universality class. The exponent z seems to be independent of the initial configuration, unlike η and (off-course) δ, and the exponents violate the hyperscaling relation Eq. (8). This is reminiscent of the situation for systems with infinitely many absorbing states where δ and η depend continuously on the density of particles in the initial configuration [19,32]. In this case a generalized scaling relation was found [32] to replace Eq. (8)

$$\delta + \beta/\nu_{\|} + \eta = z/2, \tag{33}$$

where δ and η no longer are constants and the scaling relation, $\delta = \beta/\nu_{\|}$, is invalid. In this case I find with $\delta = 0$, $\beta/\nu_{\|} = \frac{2}{7}$, and $z = \frac{8}{7}$ that $\eta = \frac{2}{7}$, which is consistent with the simulation results.

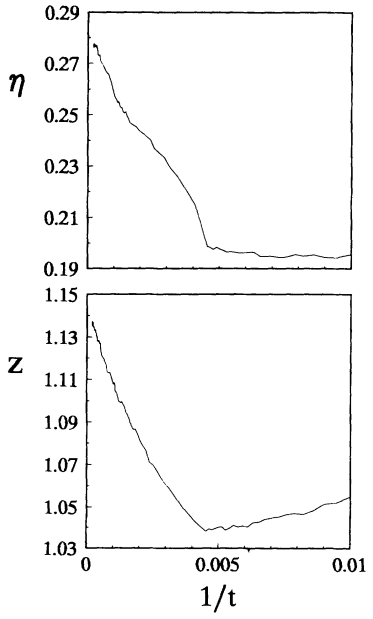

FIG. 16. Local slopes $\eta(t)$ and $z(t)$ at $p = 0.7215$ starting with a single particle.

Recently, Kim and Park studied a one-dimensional monomer-dimer model with repulsive interactions between species of the same kind [33]. When the interactions are infinitely strong (exclusion) Monte Carlo simulations showed a critical behavior consistent with the BAW with four offspring. In this version of the interacting monomer-dimer model (IMD) a monomer (A) can adsorb at an empty site only when both nearest neighbors are not occupied by a monomer. Likewise, a dimer (B_2) can adsorb and dissociate onto a pair of vacancies provided the nearest neighbors contain no B particles. There is no mutual exclusion between A and B particles. When AB pairs are formed they react immediately and the product desorbs leaving behind two empty sites. Any state concatenated from strings of sites in the form $A*A*$, $A*B*$, and $A*BB*$ (where $*$ indicates an empty site) is absorbing. The IMD has been studied using both finite-size scaling [33] and time-dependent simulations [34]. The results for various exponents are summarized in Table I. As can be seen the critical exponents for the IMD agree fully with those of the BAW with $n = 4$ showing that the IMD is in the same universality class as the BAW with four offspring.

Why does the IMD have the same critical behavior as the BAW with an even number of offspring and the "kink-models" of Grassberger *et al.*? The likely answer is that in all of these models the critical dynamics is governed by the evolution (creation or annihilation) of domain walls between absorbing regions. This point was stessed by Grassberger *et al.* [28] in their analysis of their cellular automata models. Note, that the BAW may be seen as directly modeling such domain walls. The IMD is obviously a more complicated model and several different types of domain walls are involved. Close to the critical point the system consists of large regions in an absorbing configuration separated by narrow boundary regions of "active" sites. So even though the different types of domain walls are not conserved modulo 2 it still seems likely that the critical behavior is determined by the process of getting rid of domain walls and (if possible) ending up

TABLE I. Simulation results and conjectured values for the critical exponents for the one-dimensional BAW with four offspring from this work and simulation results for the interacting monomer-dimer model from Refs. [33,34]. η' is the exponent governing the growth of the average number of particles when the absorbing can not be reached. For comparison, the corresponding exponent estimates for models in the DP universality class is listed, taken from Refs. [22,35] (β), [36] (γ, $\nu_\parallel$, and $\nu_\perp$), and [37] (δ_h). In the estimate for γ I used $\gamma = \gamma^{\rm DP} - \nu_\parallel$. The estimates for the remaining exponents were obtained using scaling relations. The figures in parenthesis are the quoted uncertainties in the last digits.

Exponent	BAW simulations	Conjecture	IMD simulations	DP class
β	0.92(3)	$\frac{13}{14}$	0.88(2)	0.2767(4)
γ	0.00(5)	0	N.A.	0.5438(13)
$\nu_\parallel$	3.25(10)	$\frac{13}{4}$	3.17(5)	1.7334(10)
$\nu_\perp$	1.84(6)	$\frac{13}{7}$	1.83(3)	1.0972(6)
$\beta/\nu_\perp$	0.500(5)	$\frac{1}{2}$	0.48(2)	0.2522(6)
$\nu_\parallel/\nu_\perp$	1.750(5)	$\frac{7}{4}$	1.734(3)	1.5798(18)
δ	0.285(2)	$\frac{2}{7}$	0.292(7)	0.1596(4)
η	0.000(1)	0	0.01(2)	0.3137(10)
η'	0.282(4)	$\frac{2}{7}$	0.28(2)	
z	1.141(2)	$\frac{8}{7}$	1.3(2)	1.2660(14)
$1/\delta_h$	0.222(2)	$\frac{2}{9}$	N.A.	0.111(3)

with just a single absorbing domain. Though the models are quite different their critical behavior may very well be governed by the same "critical domain dynamics," which would explain why the models exhibit the same critical behavior. These arguments are obviously not rigorous, but still may provide some insight into why these models apparently belong to the same universality class.

VII. SUMMARY

The critical exponents of the BAW with an even number of offspring have been determined accurately and could be given exactly by simple rational numbers listed in Table I. This model clearly belongs to a non-DP universality class. I have argued that the cellular automata models, proposed by Grassberger *et al.* [28], for the dynamics of kinks between ordered (absorbing) states and a recently proposed interacting monomer-dimer model [33] also belong to this universality class. The novel non-DP critical behavior is apparently associated with the process of eliminating domain walls (kinks) in order to end up with a single absorbing domain.

ACKNOWLEDGMENTS

I am grateful to M. H. Kim and H. Park for communicating their results prior to publication. I would like to thank R. Dickman and H. Park for interesting and enlightening discussions on the BAW and IMD models. Financial support from the Australian Research Council is gratefully acknowledged.

[1] Several articles about directed percolation may be found in *Percolation Structures and Processes*, edited by G. Deutscher, R. Zallen, and J. Adler, Annals of the Israel Physical Society, Vol. 5 (Hilger, Bristol, 1983).
[2] J. L. Cardy and R. L. Sugar, J. Phys. A **13**, L423 (1980).
[3] H. K. Janssen, Z. Phys. B **58**, 311 (1985).
[4] P. Grassberger, J. Phys. A **22**, 3673 (1989).
[5] T. E. Harris, Ann. Prob. **2**, 969 (1974).
[6] T. M. Liggett, *Interacting Particle Systems* (Springer-Verlag, New York, 1985).
[7] R. Durrett, *Lecture Notes on Particle Systems and Percolation* (Wadsworth Publishing Co., Pacific Grove, CA, 1988).
[8] F. Schlögl, Z. Phys. B **253**, 147 (1972).
[9] P. Grassberger and A. de la Torre, Ann. Phys. (New York) **122**, 373 (1979).

[10] H. K. Janssen, Z. Phys. B **42**, 151 (1981).
[11] P. Grassberger, Z. Phys. B **47**, 365 (1982).
[12] R. C. Brower, M. A. Furman, and M. Moshe, Phys. Lett. B **76**, 213 (1978).
[13] R. Bidaux, N. Boccara, and H. Chaté, Phys. Rev. A **39**, 3094 (1989); I. Jensen, *ibid.* **43**, 3187 (1991).
[14] T. Aukrust, D. A. Browne, and I. Webman, Phys. Rev. A **41**, 5294 (1990).
[15] R. Dickman, Phys. Rev. A **42**, 6985 (1990).
[16] R. Dickman and Tania Tomé, Phys. Rev. A **44**, 4833 (1991).
[17] R. Dickman, Phys. Rev. B **40**, 7005 (1989).
[18] R. M. Ziff, E. Gulari, and Y. Barshad, Phys. Rev. Lett. **56**, 2553 (1986); G. Grinstein, Z.-W. Lai, and D. A. Browne, Phys. Rev. A **40**, 4820 (1989); I. Jensen, H. C. Fogedby, and R. Dickman, *ibid.* **41**, 3411 (1990).
[19] I. Jensen, Phys. Rev. Lett. **70**, 1465 (1993); I. Jensen and R. Dickman, Phys. Rev. E. **48**, 1710 (1993).
[20] H. Takayasu and A. Yu. Tretyakov, Phys. Rev. Lett. **68**, 3060 (1992).
[21] M. Bramson and L. Gray, Z. Warsch. verw. Gebiete **68**, 447 (1985).
[22] I. Jensen and R. Dickman, J. Stat. Phys. **71**, 89 (1993).
[23] I. Jensen, Phys. Rev. E **47**, R1 (1993).
[24] N. Inui, Phys. Lett. A **184**, 79 (1993).
[25] M. Suzuki, J. Phys. Soc. Jpn. **55**, 4205 (1986); M. Suzuki, M. Katori, and X. Hu, *ibid.* **56**, 3092 (1987); M. Katori and M. Suzuki, *ibid.* **56**, 3113 (1987).
[26] A. Sudbury, Ann. Probab. **18**, 581 (1990).
[27] H. Takayasu and N. Inui, J. Phys. A **25**, L585 (1992).
[28] P. Grassberger, F. Krause, and T. von der Twer, J. Phys. A **17**, L105 (1984); P. Grassberger, *ibid.* **22**, L1103 (1989).
[29] I. Jensen, J. Phys. A **26**, 3921 (1993).
[30] I. Jensen, Phys. Rev. A **46**, 7393 (1992).
[31] M. E. Fisher, in *Critical Phenomena*, Proceedings of the International School of Physics "Enrico Fermi," Course LI, Varenna, 1971, Vol. 51, edited by M. S. Green (Academic Press, Varenna, Italy, 1971); M. N. Barber, in *Phase Transitions and Critical Phenomena, Vol. 8*, edited by C. Domb and J. L. Lebowitz (Academic Press, New York, 1983); *Finite Size Scaling and Numerical Simulations of Statistical Systems*, edited by V. Privman (World Scientific, Singapore, 1990).
[32] J. F. F. Mendes, R. Dickman, M. Henkel, and M. C. Marques, J. Phys. A **27**, 3019 (1994).
[33] M. H. Kim and H. Park (unpublished).
[34] H. Park (private communication).
[35] R. J. Baxter and A. J. Guttmann, J. Phys. A **21**, 3193 (1988).
[36] J. W. Essam, K. De'Bell, J. Adler, and F. M. Bhatti, Phys. Rev. B **33**, 1982 (1986); J. W. Essam, A. J. Guttmann, and K. De'Bell, J. Phys. A **21**, 3815 (1988).
[37] J. Adler and J. A. M. S. Duarte, Phys. Rev. B **35**, 7046 (1987).